American Mineralogist, Volume 69, pages 339–348, 1984

Ferric iron in sapphirine: a Mössbauer spectroscopic study

G. Steffen, F. Seifert

Mineralogisches Institut der Universität, Kiel, Germany

and G. Amthauer

Mineralogisches Institut der Universität, Marburg, Germany

Abstract

Substitution of ferric iron for aluminum in the sapphirine structure extends up to an approximate composition $Mg_{3.5}Fe^{3+}_{0.7}Al_{8.3}Si_{1.5}O_{20}$ at 1150°C, 2 kbar and high oxygen fugacities. The sapphirines coexist with Fe^{3+}-bearing corundum, Fe^{3+}-bearing spinels and cordierite. By comparing the hyperfine parameters of ^{57}Fe in sapphirine with those reported for other crystal structures, Fe^{3+} is assigned to the tetrahedral positions in sapphirine. It is distributed largely statistically over the different tetrahedral sites, possibly with the exception of the small T2 site. Given high oxygen fugacities, ferric iron contents in sapphirines are expected to increase up to a limiting pressure on the order of 10 kbar and then decrease with greater pressures.

Introduction

Natural sapphirines can essentially be described in the system $MgO–FeO–Al_2O_3–Fe_2O_3–SiO_2$. Nearly all experimental studies have, however, modeled sapphirine in the system $MgO–Al_2O_3–SiO_2$, where its composition may lie within the approximate limits $2MgO \cdot 2Al_2O_3 \cdot SiO_2$ and $7MgO \cdot 9Al_2O_3 \cdot 3SiO_2$ (substitution $2Al \rightleftharpoons Mg+Si$). Natural sapphirines exhibit in addition the substitutions $Mg \rightleftharpoons Fe^{2+}$ and $Al \rightleftharpoons Fe^{3+}$. Although the two Fe-free end members account for some 75 to 95 per cent of the composition of natural sapphirines, the incorporation of either ferrous or ferric iron or both may affect the phase relationships of sapphirine significantly. For example, Seifert (1974), comparing natural sapphirine-bearing assemblages to those encountered in the $MgO–Al_2O_3–SiO_2–H_2O$ system, argued that most of the discrepancies between the two sets of data could be due to the presence of Fe^{2+} in natural sapphirines and its coexisting minerals. Caporuscio and Morse (1978) suggested that the stability range of the petrologically important sapphirine + quartz assemblage might be greatly enhanced by the incorporation of ferric iron into the sapphirine structure.

As a first step towards solving these problems Fe^{3+}-bearing sapphirines have been studied here.

Experimental methods

The compositions studied were $Mg_{3.5}Al_{9-x}Fe^{3+}_xSi_{1.5}O_{20}$ with x = 0.2, 0.4, 0.6, and 0.8, encompassing the Fe^{3+} contents observed in most natural sapphirines. The Si/R^{3+} ratio of 3:18 was chosen because sapphirines have a similar ratio at high temperature and low pressure (*cf.* Higgins *et al.*, 1979). These bulk compositions were prepared as gels (Hamilton and Henderson, 1968). Most of the synthesis runs were done in an internally-heated autoclave at a pressure of 2 kbar and a temperature of 1150°C. The oxygen fugacity was kept high by either adding PtO_2 to the charges or buffering with the $MnO_2–Mn_2O_3$ buffer.

Mössbauer spectra were taken in constant acceleration mode with a ^{57}Co in Rh source of 30 mCi activity. Recording and fitting procedures were identical to those applied by Seifert and Olesch (1977) and Amthauer *et al.* (1976). All isomer shifts are reported relative to metallic iron. Lattice constants were determined by a least squares technique (Burnham, 1962) from powder diffractograms with Si as internal standard, with an indexing based on a monoclinic cell (Borg and Smith, 1969).

Results of syntheses

At 1150°C, 2 kbar and 100 hours run duration high yields of sapphirine were obtained when starting from gels with x = 0.2, 0.4 and 0.6, with only traces (about 3%) of corundum and spinel. At x = 0.8, however, additional cordierite appeared and the amount of sapphirine had decreased. The phase relationships as well as the variation of physical properties (Table 1) with composition suggest that the limit of solid solubility in synthesis runs under the chosen conditions of pressure and temperature lies between 0.6 and 0.8 Fe^{3+} per formula unit.

The composition of corundum and spinel coexisting in small amounts with sapphirine has been deduced from the lattice constants (Steinwehr, 1967; Sharma *et al.*, 1973).

0003–004X/84/0304–0339$02.00

Table 1. Lattice constants and mean refractive indices of sapphirines, $Mg_{3.5}Fe_xAl_{9-x}Si_{1.5}O_{20}$, synthesized at 1150°C, 2 kbar

x	0.0	0.2	0.4	0.6	0.8
a_o (Å)	11.286(7)	11.293(7)	11.301(9)	11.306(7)	11.322(10)
b_o	14.393(5)	14.413(9)	14.430(5)	14.437(8)	14.445(6)
c_o	9.947(6)	9.956(6)	9.969(7)	9.977(6)	9.976(7)
β (degrees)	125.46(3)	125.45(3)	125.53(4)	125.44(3)	125.51(4)
V_o (Å^3)	1316(2)	1320(2)	1323(2)	1327(2)	1328(3)
n	44	41	32	39	34
n_m	1.712(5)	1.717(5)	1.725(5)	not det.	1.743(5)

n = number of reflections used in the least-squares refinement
n_m = mean refractive index
Parenthesized figures represent one estimated standard deviation in terms of least units cited for the value to their immediate left, thus 11.286(7) indicates a standard deviation of 0.007.

The hematite concentration in the corundum phase is small at low x (1.6±0.8 mole% Fe_2O_3 at x = 0.2) but increases with x (6±1% Fe_2O_3 at x = 0.6 and 5±1% at x = 0.8). The latter values lie close to the maximum solid solubility of Fe_2O_3 in Al_2O_3 at the temperature employed (about 7 mole%, Muan, 1958). The spinel phase exhibits nearly constant *a* values indicating $MgFe_2O_4$ concentrations of the order of 1 ($x \leq 0.4$) to 3 mole% (at $x > 0.4$).

Analysis of phase relations (Fig. 1b) suggests that the appearance of small amounts of corundum and spinel solid solutions besides sapphirine mixed crystals at Fe^{3+} contents up to 0.6 Fe^{3+} per formula unit is due to preferential leaching of SiO_2 from the charges by the coexisting hydrous vapor phase and/or to a shift in composition of the sapphirines from the $7MgO \cdot 9(Al,Fe)_2O_3 \cdot 3SiO_2$ join towards the $2MgO \cdot 2(Al,Fe)_2O_3 \cdot SiO_2$ join. The $Fe^{3+}/(Fe^{3+}+Al)$ ratios of the bulk composition, of the corundum and the spinel phase indicate that ferric iron and alumina are not strongly fractionated. This and the high modal amount of sapphirine are strong evidence that the $Fe^{3+}/(Fe^{3+}+Al)$ ratio in the sapphirines is very close to that of the starting material.

At Fe^{3+} contents above 0.6 per formula unit the join studied enters a four-phase volume formed by sapphirine solid solution with maximum Fe^{3+} content (about 0.7 Fe^{3+} according to the variation of physical properties, Table 1), a corundum mixed crystal ($Fe^{3+}/(Fe^{3+}+Al)$ about 0.06), spinel ($Fe^{3+}/(Fe^{3+}+Al) = 0.03$), and cordierite. These relations can only be consistent if the cordierite has a $Fe^{3+}/(Fe^{3+}+Al)$ ratio of about 0.15. This value is higher than that encountered in most natural cordierites (generally below 0.06, Schreyer, 1965) but can still be considered plausible at the high temperatures and oxygen fugacities employed.

Mössbauer study of ^{57}Fe in synthetic sapphirine

Synthetic sapphirines of nominal composition $Mg_{3.5}Al_{9-x}Fe_xSi_{1.5}O_{20}$ with x = 0.2, 0.4 and 0.6 have been investigated by Mössbauer spectroscopy at room temperature, 77 K and 4.2 K. All spectra exhibit two broad but well resolved peaks of nearly equal intensity at velocities in the vicinity of −0.2 and +0.7 mm/sec, respectively. In some spectra a very weak peak at a velocity around 2 mm/sec could be recognized (Fig. 2). It is clear from these line positions that the strong doublet is due to ferric iron whereas the weak peak represents the high velocity component of a ferrous doublet. The area ratio indicates that more than 95% of the total iron is in the ferric state and ferrous iron will, therefore, be neglected in the following.

In all the spectra there is an asymmetry of the line widths and intensities (*cf.* Table 2). This asymmetry may be caused either by a close overlap of several doublets with slightly different isomer shifts and quadrupole splittings or/and an asymmetry of a doublet. The latter could be due to (1) texture in the crystal orientation of the polycrystalline absorber, (2) anisotropic recoilless fraction (Goldanskii–Karyagin effect) or (3) paramagnetic relaxation.

The asymmetry of the lines did not change in spectra taken with different orientations of the absorber to the incident gamma-rays and therefore texture effects have only a minor influence on the shape of the spectra. In the case of anisotropic recoilless fraction the asymmetry should vanish approaching the zero point of the temperature scale. This is not observed in the low temperature spectra and for that reason any important influence from the Goldanskii–Karyagin effect can be eliminated. The asymmetry in line width, observed in the x = 0.2 spectrum (Table 2), diminishes with increasing Fe content. This behavior suggests electronic spin–spin relaxation due to the wide separation of the Fe^{3+} atoms in the low-Fe sapphirines but absence of such effects in the x = 0.6 sample. The latter sample does not show increasing asymmetry of the lines at decreasing temperatures and therefore has no spinlattice relaxation as expected for

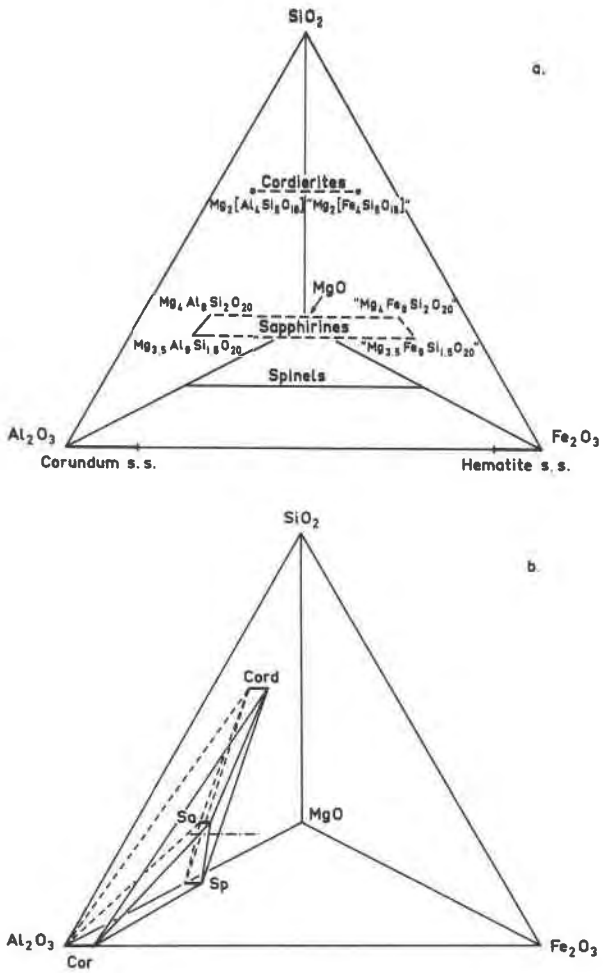

Fig. 1. a. Phases in the system $MgO–Al_2O_3–Fe_2O_3–SiO_2$ pertaining to the present study. The approximate solid solubilities on the $Al_2O_3–Fe_2O_3$ join are taken from Muan (1958). Ternary miscibility in the spinels has been neglected. The miscibility shown for sapphirine (based on the substitutions $2Al \rightleftharpoons Mg+Si$ and $Fe^{3+} \rightleftharpoons Al$) and for cordierite (substitution $Fe^{3+} \rightleftharpoons Al$) is hypothetical. b. Schematic phase relations in part of the system $MgO–Al_2O_3–Fe_2O_3–SiO_2$ at 1150°C, 2 kbar. The dash-dotted line gives the join studied. Dashed tie lines refer to the limiting system $MgO–Al_2O_3–SiO_2$ (*cf.* Seifert, 1974). For discussion see text.

Fe^{3+} with its electronic ^6s state and vanishing orbital momentum (Blume, 1965). Even the application of a small magnetic field of 0.5 kG at 4.2 K absorber temperature did not affect the line shape indicating the absence of relaxation phenomena in the x = 0.6 sample.

The apparent asymmetry of the lines can thus most probably be referred to the existence of several quadrupole doublets assigned to different lattice sites, whose low velocity components strongly overlap and whose high velocity components are more separated. In the following we will concentrate on the evaluation of the x = 0.6 spectra and, in the absence of pronounced relaxation effects, assume a Lorentzian line shape.

Fitting only one doublet for ferric iron led to unacceptable line widths (Table 2). Inserting two doublets without any constraints into the x = 0.6 spectra at 298 K and 77 K, which were statistically rather good, produced the hyperfine parameters given in Table 3 (*cf.* Fig. 2). The line widths are still too high for one position per doublet but the residuals are evenly distributed. The isomer shifts of both doublets are almost identical and exhibit the normal temperature dependence, which has to be referred to the second order Doppler shift. The quadrupole splittings are distinctly different and almost independent of temperature as expected for Fe^{3+}. Interchanging the positions of the high velocity lines of both doublets was possible only when widths and intensities for one doublet were constrained to be equal. This fitting procedure led, for the 298 K spectrum, to a doublet with a lower (IS =

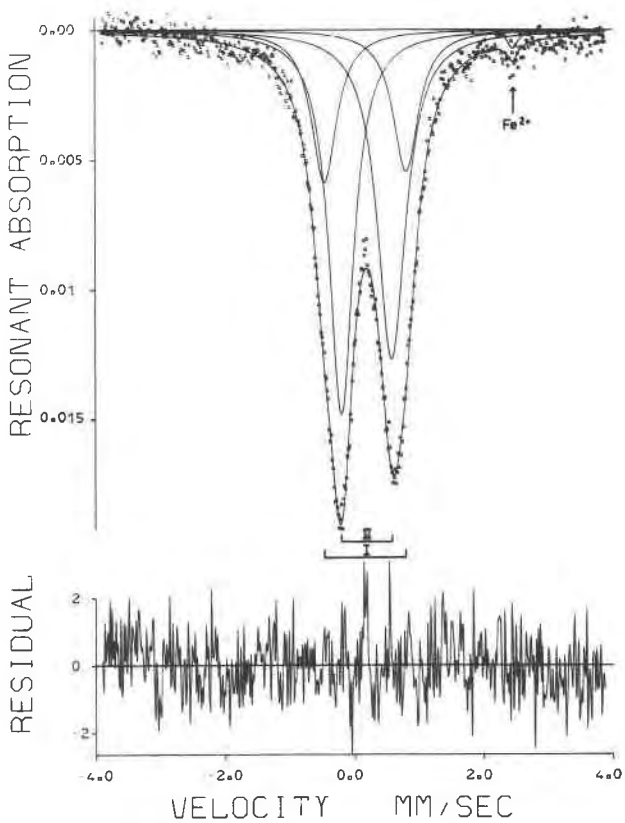

Fig. 2. Mössbauer spectrum of synthetic sapphirine of nominal composition $Mg_{3.5}Fe_{0.6}Al_{8.4}Si_{1.5}O_{20}$ fitted to five unconstrained Lorentzians (fifteen line variables, one background variable). The peak labeled Fe^{2+} is the high-velocity component of a weak ferrous doublet. Doublets I and II are due to ferric iron. The deviation of the sum curve of all Lorentzians from the data, divided by the square root of the background, is plotted as residual below the spectrum.

Table 2. Hyperfine parameters of ferric iron in sapphirine (two-line fits)

x	0.2	0.4	0.6	0.6	0.6	0.6+
T	298	298	298	77	4.2	4.2
I1	0.522	0.523	0.534	0.522	0.516	0.512
B_H	1.14	0.99	0.58	0.64	0.76	0.80
B_L	0.73	0.89	0.59	0.62	0.71	0.79
QS	0.95	1.18	0.91	0.91	0.92	0.94
IS	0.28	0.32	0.30	0.36	0.39	0.38

x = number of Fe^{3+} atoms per 20 oxygens
T = absorber temperature in K
I1 = fractional intensity of the low-velocity component
B_H, B_L = full widths at half intensity, in mm/sec. The subscripts H and L refer to the high- and low-velocity components of the doublets, respectively.
QS = quadrupole splitting in mm/sec (± 0.04 at x = 0.2 and 0.4, ± 0.02 at x = 0.6)
IS = isomer shift in mm/sec, relative to metallic iron (± 0.04 at x = 0.2 and 0.4, ± 0.02 at x = 0.6)
+ = taken in a magnetic field of 500 G, in the direction of the γ-rays

0.15 mm/sec, QS = 0.81 mm/sec) and a doublet with a larger isomer shift (IS = 0.36 mm/sec, QS = 0.89 mm/sec), which might be assigned to the tetrahedral and octahedral sites, respectively. However, this fit was not stable at all when releasing the constraints, as required by the asymmetry of the lines. In addition, the low octahedral isomer shift and quadrupole splitting are not in agreement with the trend usually observed, where low isomer shifts are always combined with large quadrupole splittings, *i.e.*, high site distortions, as will be discussed below. Therefore, this fitting procedure was considered to be unrealistic and was not considered further. In attempts to insert a third doublet the fit had to be heavily constrained and the goodness of fit parameters, chi^2 and misfit (Ruby, 1973), were not significantly improved. We thus conclude that a two-doublet fit as reported in Table 3 can be justified by the data and that Fe^{3+} is present in more than one position.

When comparing our room-temperature data to those of Bancroft *et al.* (1968) for yellow (only Fe^{3+}-bearing) sapphirine (Table 3) it is evident that the hyperfine parameters of the two spectra are very similar. In particular, the isomer shifts are nearly identical.

Discussion and conclusions

Previous studies on the structural role of Fe^{3+} in sapphirine

The basic sapphirine structure may be described as consisting of branched T_6O_{18} (T = Si,Al) chains with six crystallographically distinct tetrahedral sites and eight different octahedral MO_6 (M = Mg,Al) sites forming walls and single octahedra (Moore, 1969). Ferric iron proxying for Al might thus enter either the tetrahedral or octahedral sites or both.

In an early Mössbauer study, Bancroft *et al.* (1968) investigated both a highly oxidized (*i.e.*, only Fe^{3+}-bearing) sapphirine as well as a ferrous- and ferric-bearing sample. On the basis of the isomer shift of ferric iron in the oxidized sample (0.27 to 0.30 mm/sec) they assigned Fe^{3+} to tetrahedral positions. Recent structure determinations of sapphirine have, however, allocated ferric iron to octahedral sites (Merlino, 1980, Higgins and Ribbe, 1979, Higgins *et al.*, 1979) and quoted a personal communication by Burns (1972) to Morse as a reference. Burns had measured 0.37 mm/sec as the isomer shift of ferric iron and cautiously concluded that most of the ferric iron was in octahedral coordination but that some could be tetrahedrally coordinated. The values reported for the isomer shift (and also the value reported in this paper) fall more or less into an intermediate range between those for octahedral and tetrahedral ferric iron (see below) and we have to be particularly concerned with the precision of the data when drawing any conclusion on the coordination of ferric iron in sapphirine. The spectrum taken by Burns showed strong absorption bands due to Fe^{2+} completely masking the low-velocity band of the Fe^{3+} doublet. Consequently, the isomer shift derived for the Fe^{3+} doublet (0.37 mm/sec) is less certain and the value obtained also depends on the number of doublets fitted for ferrous iron (Burns, pers. comm., 1981). Statistical analysis of Burns' data with the procedure of Dollase (1975) suggests that the isomer shift reported may well be off by 0.1 mm/sec because the low-velocity Fe^{3+} and the strongest Fe^{2+} peaks are only separated by about 0.25 half widths.

After this study was completed, Merlino (pers. comm., 1981) re-refined the structure of 1Tc sapphirine from Wilson Lake and tried to allocate ferric iron to tetrahedral sites. In the refinement iron was rejected from these sites. However, the composition obtained from the X-ray refinement showed poor agreement with the chemical anal-

Table 3. Hyperfine parameters of ^{57}Fe in synthetic sapphirine (composition $Mg_{3.5}Fe^{3+}_{0.6}Al_{8.4}Si_{1.5}O_{20}$) at 77 K and room temperature, compared to those of natural sapphirine (Bancroft *et al.*, 1968, yellow sample)

	synthetic sapphirine				natural sapphirine	
	77 K		RT		RT	
	Doubl.I	Doubl.II	Doubl.I	Doubl.II	Doubl.I	Doubl.II
IS	0.34	0.37	0.29	0.30	0.27	0.30
QS	1.21	0.78	1.23	0.76	1.37	0.78
B_H	0.58	0.56	0.53	0.45	0.73	0.52
B_L	0.47	0.48	0.48	0.49	0.59	0.52
Area	0.35	0.65	0.36	0.64	0.42	0.58

IS = isomer shift in mm/sec, relative to metallic iron (± 0.02)
QS = quadrupole splitting in mm/sec (± 0.02)
B_H, B_L = full widths at half intensity, in mm/sec. The subscripts H and L refer to the high- and low-velocity components of the doublets, respectively.
Area = fractional areas of the doublets

ysis (0.72 Fe per 20 oxygens versus 1.08 Fe according to Merlino, 1973). An independent refinement by H. P. Weber (pers. comm., 1981) indicated that the limit of error for site occupanices in such a complicated structure is of the same magnitude as the maximum concentration of iron that could theoretically be expected on a tetrahedral site and we, therefore, conclude that no clear-cut decision on the incorporation of these rather low amounts of ferric iron into either tetrahedral or octahedral sites can be made on the basis of X-ray diffraction.

Octahedral versus tetrahedral Fe^{3+} in sapphirine

The isomer shifts of 0.29 and 0.30 mm/sec for Fe^{3+} (at room temperature) in sapphirine reported in this paper fall into the gap between the values found at room temperature for most compounds with Fe^{3+} in tetrahedral coordination (0.17 to 0.26 mm/sec, Annersten and Hålenius, 1976) and those with Fe^{3+} in octahedral coordination (0.36 to 0.50 mm/sec) and any attempts to localize the ferric iron in the sapphirine structure on the basis of Mössbauer spectra has to rationalize this anomalous behavior.

Low isomer shifts for ferric iron in octahedral coordination have been reported for epidote (M3 position, 0.35–0.36 mm/sec, Dollase, 1973) and braunite (0.35 mm/sec, Seifert and Dasgupta, 1982) and they are connected with large quadrupole splittings (2.06–2.10 and 1.91–2.10 mm/sec, respectively). These Fe^{3+}-containing sites are highly distorted. Using the format of calculation given by Fleet (1976) and from the structural data given by Dollase (1971) and Moore and Araki (1976) bond length distortion parameters of 0.0047 are obtained for the M3 position in epidote and 0.0048 to 0.0059 for the Mn2 to Mn4 positions in braunite. From the low quadrupole splitting of ferric iron in sapphirine (0.76 and 1.23 mm/sec for the two doublets) and from the small distortion of the octahedral sites (bond length variation 0.0001 to 0.0007, calculated from the X-ray data given by Higgins and Ribbe, 1979) it is concluded that the hyperfine parameters of ferric iron cannot be explained by an anomalous octahedral coordination. This is further supported by the isomer shift of ferric iron in octahedral coordination in aenigmatite which is structurally closely related to sapphirine (IS = 0.41, QS = 0.58 mm/sec at room temperature, Seifert, unpublished data).

On the other hand, it has been suggested empirically (Annersten and Hålenius, 1976, Annersten and Olesch, 1978), and has later been confirmed by molecular orbital calculations (Tang Kai *et al.*, 1980) that the isomer shift of tetrahedral ferric iron increases strongly with the average metal-anion distance of the positions involved. Large tetrahedral bond lengths could, therefore, explain the isomer shifts encountered in sapphirine.

Table 4 gives geometrical parameters for the tetrahedral sites in the sapphirine structure. A complete compilation of all data available for ferric iron in tetrahedral coordination is presented in Table 5. Considering the relationship between isomer shift and average cation-oxygen bond length (Fig. 3), the data cluster clearly into two groups, each of which show a positive correlation, but different slopes. The group of points at rather low R (1.6–1.75Å) represents crystal structures with only small Fe^{3+} concentrations in tetrahedral sites, *i.e.*, the averaged R values determined by X-ray (or neutron) diffraction are mostly governed by the smaller cation for with Fe^{3+} is proxying. The data points in the range 1.85 to 1.95Å, on the other hand, represent structures with large mole fractions of Fe^{3+} on the sites considered, *i.e.*, a site geometry largely reflecting the properties of ferric iron.

Table 4. Average bond lengths, bond length distortion and bond angle variation parameters of tetrahedra in the sapphirine structure, calculated from data reported by Higgins and Ribbe (1979)

	T1	T2	T3	T4	T5	T6
$\bar{R}$	1.752	1.647	1.716	1.759	1.760	1.734
$\Delta \cdot 10^4$	1.54	0.98	1.26	3.63	3.78	0.90
σ^2	7.80	1.67	4.19	14.15	14.84	14.94
Al	0.92	0.01	0.51	0.92	1.00	0.73

Δ = bond length distortion = $\frac{1}{4}\sum_{i=1}^{4}((R_i-\bar{R})/\bar{R})^2$ (Fleet 1976)

σ^2 = bond angle variation = $\frac{1}{5}\sum_{i=1}^{6}(\Theta_i-109.5)^2$ (Robinson et al. 1971)

$\bar{R}$ = average cation - oxygen bond length (Å)

Al = Al content of tetrahedra according to Higgins and Ribbe (1979)

R_i = individual cation - oxygen bond length (Å)

Θ_i = individual oxygen - cation - oxygen bond angle (degrees)

It can be seen from Figure 3 that the isomer shift of the Fe^{3+} doublets encountered in sapphirine are consistent with a tetrahedral coordination and that the anomalously high value for such a coordination is due to the large average bond length of the tetrahedra into which Fe^{3+} substitutes. Therefore it has to be concluded on the basis of the Mössbauer results of this study that most of the Fe^{3+} enters the tetrahedral sites of the sapphirine structure and only a minor portion could be located at the octahedral sites. This is surprising because in many other silicates as for example the garnets (Huggins *et al.*, 1977) Al and Fe^{3+} are distributed over the tetrahedral and octahedral sites in the case of silicon deficiency and Al exhibits the stronger tetrahedral site preference. The availability of large tetrahedra in the sapphirine structure might be the cause of the different Al–Fe^{3+} ordering scheme.

The relationships between other structural and hyperfine parameters (Table 5) are not well defined. In theory, the quadrupole splitting for ferric iron has to increase with increasing distortion (*e.g.*, Bancroft, 1973) and it does so with either distortion parameter defined and

Table 5. Structural data and hyperfine parameters of phases with Fe^{3+} in tetrahedral coordination

No.		$\bar{R}$ (Å)	$\Delta \cdot 10^4$	σ^2	IS	QS	Reference
1	$Bi_3(FeO_4)(MoO_4)_2$	1.909	1.045	81.164	0.28	1.04	Jeitschko et al. (1976)
2	Xanthophyllite	1.730	0.836	3.144	0.27 0.24 0.26 0.24	0.62 0.68 0.65 0.80	Takéuchi (1965), Annersten and Olesch (1978)
3	$Bi_2Fe_4O_9$	1.880	6.437	9.486	0.24	0.96	Niizeki and Wachi (1968), Kostiner and Shoemaker (1971)
4	Diopside	1.663	3.005	23.812	0.14 0.17 0.18	1.62 1.54 1.49	Peacor (1967), Hafner and Huckenholz (1971)
5	Orthopyroxene	1.634 1.623 1.629	6.065 2.241	18.170 29.234	0.18 0.21	1.34 1.34	Ghose (1965), Annersten et al. (1978)
6	Orthoclase	1.652 1.633 1.643	0.009 0.114	9.938 6.764	0.21 0.22	0.48 0.61 0.65	Jones and Taylor (1961), Annersten (1976)
7	$Ca_2Fe_2O_5$	1.878	3.368	45.602	0.20	1.38	Colville (1970), Geller et al. (1970)
8	$Y_3Fe_5O_{12}$	1.866	0	84.300	0.16	1.03	Euler and Bruce (1965), Belozerskii et al. (1970)
9	$CuFe_2O_4$	1.890	0	0.040	0.27[b]	0.04[b]	Evans and Hafner (1968)
10	Phlogopite	1.681	0.231	1.438*	0.19 0.21	0.44 0.44	Steinfink (1962), Hogarth et al. (1970)
11	$Sr_2Fe_2O_5$	1.874[a]	0.918	152.600	0.18	n.d.	Greaves et al. (1975), Gallagher et al. (1964)
12	ß-$NaFeO_2$	1.860	1.373	n.d.	0.18	n.d.	Bertaut et al. (1963), Birchall et al. (1969)
13	Ti-andradite	1.744[a]*	0*	35.215*	0.20	1.15	Weber et al. (1975), Amthauer et al. (1976)
14	$CsFeSi_2O_6$	1.632*	0.903*	3.612*	0.21	0.51	Kopp et al. (1963), Kume and Koizumi (1965), Birchall et al. (1969)
15	Magnetite	1.920	0*	0*	0.27	0	Fagherazzi and Garbassi (1971), Häggström et al. (1978)

$\bar{R}$ = average cation - oxygen bond length
Δ_2 = bond length distortion (Fleet 1976)
σ^2 = bond angle variation (Robinson et al., 1971)
IS = isomer shift, relative to metallic iron, in mm/sec, at room temperature
QS = quadrupole splitting, in mm/sec, at room temperature (absolute value)
n.d. = no data available
a: determined from neutron diffraction data, all others from X-ray diffraction
b: H_{eff} = 481 kOe
In the column "Reference" the article referring to the structure determination is cited first and that reporting the hyperfine parameters last.
* = calculated from the data given in the reference

given in Table 5 but the scatter is considerable (Fig. 4 a,b). These poor correlations could be due to one or several of the following effects: (1) the geometrical parameters are averages for any crystallographically distinct site and do not necessarily reflect the geometry of a specific position occupied by Fe^{3+} (*cf.* above). (2) The electrical field gradient that determines the quadrupole splitting is not strictly described by the purely geometrical parameters based on the mean positions. (3) None of the distortion parameters employed is in itself sufficient to describe polyhedral distortion (Fleet, 1976). It should be emphasized, however, that the parameters for sapphirine fit the general trends and do not contradict the allocation of Fe^{3+} to the tetrahedral positions (Fig. 4).

Ordering of Fe^{3+} over tetrahedral positions

It has been deduced above that Fe^{3+} enters at least two different groups of tetrahedral positions in the sapphirine structure. The significant differences in the quadrupole splittings of the two doublets suggest that these groups of positions differ in distortion. We assign the weaker outer doublet to Fe^{3+} in a more distorted environment (*cf.* Fig. 4a,b).

The distortion parameters of the tetrahedra in the sapphirine structure are compiled in Table 4 and plotted as histograms in Figure 5. Clearly, the tetrahedra T4 and T5 are highly distorted and T1, T2, T3 are little distorted, irrespective of the distortion parameter used, whereas T6

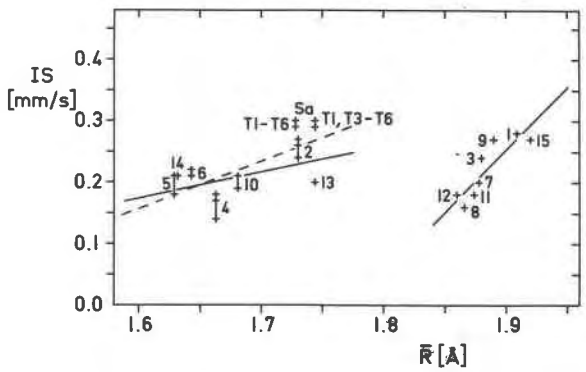

Fig. 3. Relationship between isomer shift (IS) of tetrahedral ferric iron and average bond length R. Numbers refer to Table 5. In cases where several structurally distinct positions may be suited for incorporation of ferric iron (*e.g.*, enstatite) only their average R has been plotted. For sapphirine, two different R averages are shown, one including, and one excluding the T2 position (*cf.* Table 4). The lengths of the bars correspond to the ranges of isomer shifts reported. For the two groups of data points regression lines have been fitted. The line for high values of R corresponds to IS = − 3.582 + 2.019 R (r^2 = 0.76), the full line at low R (not including the values for sapphirine), IS = − 0.515 + 0.431 R (r^2 = 0.26), whereas the dashed line, IS = − 1.079 + 0.772 R (r^2 = 0.50), includes the indicated values of sapphirine. For discussion see text.

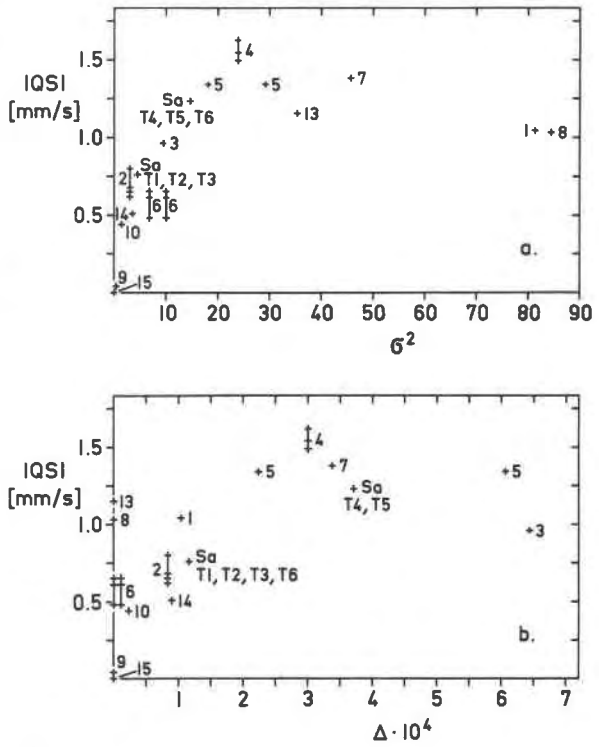

Fig. 4. Relationship between quadrupole splitting (QS) of tetrahedral ferric iron and the distortion parameters, bond angle variation σ^2 (a) and bond length distortion Δ (b), based on the data given in Table 5. Where more than one structurally distinct position may be suited for incorporation of ferric iron, their geometrical parameters have been plotted separately. The data for sapphirine have also been plotted with the band assignment derived in the text (*cf.* Tables 2 and 4).

cannot be unambigously assigned. Incorporation of ferric iron into the T2 site might be considered improbable, both because of the small size of this position and the absence of a doublet with low isomer shift.

The area ratio of the doublet with the larger quadrupole splitting (corresponding to Fe^{3+} in a group of sites with large distortion) to the total intensity observed is 0.36 at 295 K for the sapphirine investigated here and 0.42 for the natural sapphirine studied by Bancroft *et al.* (1968). These ratios are consistent with a statistical (*i.e.*, random) distribution of ferric iron if we take the bond length variation as discriminant parameter for distortion. The precision of the data is not high enough to ascertain the incorporation of ferric iron into the T2 site.

From these considerations and from the line widths of the doublets it is concluded that ferric iron substitutes randomly in the tetrahedral sites, possibly with the exception of the T2 site, in both the synthetic of this study and the natural sample of Bancroft *et al.* (1968). Exchange processes involving ferric iron are either too slow or energetic differences between the sites are too small to produce significant ordering even within geologic time periods.

Solid solubility of Fe^{3+}-sapphirine and pressure effects

The maximum incorporation of ferric iron into sapphirine found here (about 0.7 Fe^{3+} per 20 oxygens) at 1150°C, 2 kbar, encompasses that generally encountered in natural sapphirines with the exception of an analysis reported by Sahama *et al.* (1974, 0.95 Fe^{3+}). Other natural sapphirines never exceed the value of 0.652 (Caporuscio and Morse, 1978).

The Fe^{3+} content of a natural sapphirine will also be controlled by the phase assemblage and oxygen fugacity besides the effects of pressure and temperature. The first

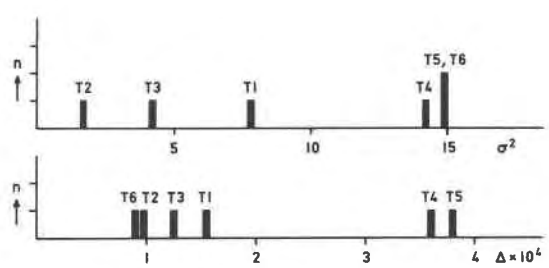

Fig. 5. Frequency distribution of tetrahedral site distortion parameters in sapphirine (*cf.* Table 2).

two factors will result in generally lower Fe^{3+} contents than those encountered here because in most natural sapphirine-bearing assemblages there is no excess of ferric iron and/or oxygen fugacities were lower than those used in the present study.

Some qualitative deductions on the effect of pressure can be made on the basis of volume properties. The change of cell volume with the incorporation of ferric iron can be used for an estimate of the molar volume of a hypothetical sapphirine end member $Mg_{3.5}Al_{4.5}Fe^{3+}_{4.5}Si_{1.5}O_{20}$, yielding 208.7 cm^3/mole to be compared with 197.0 cm^3/mole for the $Mg_{3.5}Al_9Si_{1.5}O_{20}$ phase (Schreyer and Seifert, 1970).

Taking the experimentally determined paragenesis of the Fe^{3+}-rich sapphirine (Fig. 1b) we can formulate a reaction

$$\underset{Fe^{3+}\text{-rich sapphirine}}{116\ Mg_{3.5}Al_{4.5}Fe^{3+}_{4.5}Si_{1.5}O_{20}} \rightleftharpoons \underset{Fe^{3+}\text{-free sapphirine}}{26\ Mg_{3.5}Al_9Si_{1.5}O_{20}} + \underset{\text{cordierite}}{27\ Mg_2Al_4Si_5O_{18}} + \underset{\text{magnesioferrite}}{261\ MgFe_2O_4} + \underset{\text{corundum}}{90\ Al_2O_3}$$

Molar volumes (*cf.* Robie *et al.*, 1966, Sharma *et al.*, 1973) indicate that the product assemblage has a volume 4.7% higher than the reactant phase and increasing pressures will thus increase the incorporation of Fe^{3+} into sapphirine in this assemblage. At high pressures where the low-density phase cordierite will no longer exist, this trend is expected to reverse. For an equilibrium of sapphirine with orthopyroxene, Fe^{3+}-bearing spinel and an iron oxide phase such as described by Morse and Talley (1971) the following model reaction might be written:

$$\underset{Fe^{3+}\text{-rich sapphirine}}{36\ Mg_{3.5}Al_{4.5}Fe^{3+}_{4.5}Si_{1.5}O_{20}} \rightleftharpoons \underset{Fe^{3+}\text{-free sapphirine}}{18\ Mg_{3.5}Al_9Si_{1.5}O_{20}} + \underset{\text{enstatite}}{27\ MgSiO_3} + \underset{\text{magnesioferrite}}{36\ MgFe_2O_4} + \underset{\text{hematite}}{45\ Fe_2O_3}$$

where the product assemblage has a volume 1.8% less than that of Fe^{3+}-rich sapphirine. We might thus expect a maximum solid solubility of Fe^{3+} in sapphirine at pressures where cordierite disappears from its assemblages. This pressure probably lies in the vicinity of 8-10 kbar (*cf.* Newton 1972) and it might not be fortuitous that several particularly Fe^{3+}-rich sapphirines (*e.g.*, McKie 1963, Merlino, 1973, Sahama *et al.*, 1974) come from rocks formed at high pressures at the base of the crust.

Acknowledgments

We thank J. Heinze and H. Frey for technical assistance and F. Liebau for helpful discussions. R. Burns kindly communicated his data on sapphirine. The manuscript was greatly improved through reviews by H. Annersten, R. Burns, K. Langer, S. Merlino, G. A. Waychunas and H. P. Weber. Support by Deutsche Forschungsgemeinschaft and Friedrich-Naumann-Stiftung is gratefully acknowledged.

References

Amthauer, G., Annersten, H. and Hafner, S. S. (1976) The Mössbauer spectrum of ^{57}Fe in silicate garnets. Zeitschrift für Kristallographie, 143, 14–55.

Annersten, H. (1976) New Mössbauer data on iron in potash feldspar. Neues Jahrbuch für Mineralogie, Monatshefte, 337–343.

Annersten, H. and Hålenius, U. (1976) Ion distribution in pink muscovite, a discussion. American Mineralogist, 61, 1045–1050.

Annersten, H. and Olesch, M. (1978) Distribution of ferrous and ferric iron in clintonite and the Mössbauer characteristics of ferric iron in tetrahedral coordination. Canadian Mineralogist, 16, 199–203.

Annersten, H., Olesch, M. and Seifert, F. (1978) Ferric iron in orthopyroxene: A Mössbauer spectroscopic study. Lithos, 11, 301–310.

Bancroft, G. M. (1973) Mössbauer Spectroscopy: An introduction for inorganic chemists and geochemists. McGraw Hill, New York.

Bancroft, G. M., Burns, R. G. and Stone, A. J. (1968) Applications of the Mössbauer effect to silicate mineralogy—II. Iron silicates of unknown and complex crystal structures. Geochimica et Cosmochimica Acta, 32, 547–559.

Belozerskii, G. N., Gitsovitch, V. N., Murin, A. N., Khimich, Y. P. and Yakolev, Y. M. (1970) Determination of the parameters of quadrupole interaction in yttrium iron garnets. Journal of Experimental and Theoretical Physics, 11, 106–108, (not seen, extracted from Zeitschrift für Kristallographie, 143, 41).

Bertaut, F., Delapalme, A. and Bassi, G. (1963) Structure magnétique de β-$NaFeO_2$. Comptes Rendus Hebdomadaires des Séances de l'Academie des Sciences, 257, 421–424.

Birchall, T., Greenwood, N. N. and Reid, A. F. (1969) Mössbauer, electron spin resonance, optical and magnetic studies of iron (III) in oxide host lattices. Journal of the Chemical Society, Section A, P3, 2382–2398.

Blume, M. (1965) Magnetic relaxation and asymmetric quadrupole doublets in the Mössbauer effect. Physical Review Letters, 14, 96–98.

Borg, I. Y. and Smith, D. K. (1969) Calculated X-ray powder patterns for silicate minerals. Geological Society of America Memoir, 122.

Burnham, C. W. (1962) Lattice constant refinement. Carnegie Institution of Washington Year Book, 61, 132–135.

Caporuscio, F. A. and Morse, S. A. (1978) Occurrence of sapphirine plus quartz at Peakskill, New York. American Journal of Science, 278, 1334–1342.

Colville, A. (1970) The crystal structure of $Ca_2Fe_2O_5$ and its relation to the nuclear electric field gradient at the iron sites. Acta Crystallographica, B26, 1469–1473.

Dollase, W. A. (1971) Refinement of the crystal structures of epidote, allanite, and hancockite, American Mineralogist, 56, 447–464.

Dollase, W. A. (1973) Mössbauer spectra and iron distribution in the epidote-group minerals. Zeitschrift für Kristallographie, 138, 41–63.

Dollase, W. A. (1975) Statistical limitations of Mössbauer spectral fitting. American Mineralogist, 60, 257–264.

Euler, F. and Bruce, J. A. (1965) Oxygen coordinates of compounds with garnet structure. Acta Crystallographica, 19, 971–978.

Evans, J. and Hafner, S. S. (1968) Mössbauer resonance of Fe^{57}

in oxidic spinels containing Cu and Fe. Journal of Physics and Chemistry of Solids, 29, 1573–1588.

Fagherazzi, G. and Garbassi, F. (1971) X-ray diffraction measurements of the cation distributions in spinel structures. Journal of Applied Crystallography, 5, 18–23.

Fleet, M. E. (1976) Distortion parameters for coordination polyhedra. Mineralogical Magazine, 40, 531–533.

Gallagher, P. K., MacChesney, J. B. and Buchanan, D.N.E. (1964) Mössbauer effect in the system $SrFeO_{2.5-3.0}$. Journal of Chemical Physics, 41, 2429–2434.

Geller, S., Grant, R. W. and Fullmer, L. D. (1970) Magnetic structures in the $Ca_2Fe_{2-x}Al_xO_5$ system. Journal of Physics and Chemistry of Solids, 31, 793–803.

Ghose, S. (1965) Mg^{2+}–Fe^{2+} order in an orthopyroxene $Mg_{0.93}Fe_{1.07}Si_2O_6$. Zeitschrift für Kristallographie, 122, 81–99.

Greaves, C., Jacobson, A. J., Tofield, B. C. and Fender, B. E. F. (1975) A powder neutron diffraction investigation of the nuclear and magnetic structure of $SrFe_2O_5$. Acta Crystallographica, B31, 641–646.

Häggström, L., Annersten, H., Ericsson, T., Wäppling, R., Karner, W. and Bjarman, S. (1978) Magnetic dipolar and electric quadrupolar effects on the Mössbauer spectra of magnetite above the Verwey transition. Hyperfine Interactions, 5, 201–214.

Hafner, S. S. and Huckenholz, H. G. (1971) Mössbauer spectrum of synthetic ferri-diopside. Nature Physical Science, 233, 9–11.

Hamilton, D. L. and Henderson, C. M. B. (1968) The preparation of silicate compositions by a gelling method. Mineralogical Magazine, 36, 832–838.

Higgins, J. B., Ribbe, P. H. and Herd, R. K. (1979) Sapphirine I. Crystal chemical contributions. Contributions to Mineralogy and Petrology, 68, 349–356.

Higgins, J. B. and Ribbe, P. H. (1979) Sapphirine II. A neutron and X-ray diffraction study of $(Mg–Al)^{VI}$ and $(Si–Al)^{IV}$ ordering in monoclinic sapphirine. Contributions to Mineralogy and Petrology, 68, 357–368.

Hogarth, D. D., Brown, F. F. and Pritchard, A. M. (1970) Biabsorption, Mössbauer spectra and chemical investigation of five phlogopite samples from Quebec. Canadian Mineralogist, 10, 710–722.

Huggins, F. E., Virgo, D. and Huckenholz, H. G. (1977) Titanium containing silicate garnets. I. The distribution of Al, Fe^{3+} and Ti^{4+} between octahedral and tetrahedral sites. American Mineralogist, 62, 475–490.

Jeitschko, W., Sleight, A. W., McClellan, W. R. and Weiher, J. F. (1976) A comprehensive study of disordered and ordered scheelite-related $Bi_3(FeO_4(MoO_4)_2$. Acta Crystallographica, B32, 1163–1170.

Jones, J. B. and Taylor, W. H. (1961) The structure of orthoclase. Acta Crystallographica, 14, 443–456.

Kopp, O. C., Harris, L. A., Clark, G. W. and Yakel, H. L. (1963) A hydrothermally synthesized iron analog of pollucite—its structure and significance. American Mineralogist, 48, 100–109.

Kostiner, E. and Shoemaker, G. L. (1971) Mössbauer effect study of $Bi_2Fe_4O_9$. Journal of Solid State Chemistry, 3, 186–189.

Kume, S. and Koizumi, M. (1965) Synthetic pollucites in the system $Cs_2O \cdot Al_2O_3 \cdot 4SiO_2$–$Cs_2O \cdot Fe_2O_3 \cdot 4SiO_2$–$H_2O$—their phase relationship and physical properties. American Mineralogist, 50, 587–592.

McKie, D. (1963) Order–disorder in sapphirine. Mineralogical Magazine, 33, 635–645.

Merlino, S. (1973) Polymorphism in sapphirine. Contributions to Mineralogy and Petrology, 41, 23–29.

Merlino, S. (1980) Crystal structure of sapphirine-1Tc. Zeitschrift für Kristallographie, 151, 91–100.

Moore, P. B. (1969) The crystal structure of sapphirine. American Mineralogist, 54, 31–49.

Moore, P. B. and Araki, T. (1976) Braunite: Its structure and relationship to bixbyite and some insights on the genealogy of fluorite derivative structures. American Mineralogist, 61, 1226–1240.

Morse, S. A. and Talley, J. H. (1971) Sapphirine reactions in deep-seated granulites near Wilson Lake, Central Labrador, Canada. Earth and Planetary Science Letters, 10, 325–328.

Muan, A. (1958) On the stability of the phase $Fe_2O_3 \cdot Al_2O_3$. American Journal of Science, 256, 413–422.

Newton, R. C. (1972) An experimental determination of the high-pressure stability limits of magnesian cordierite under wet and dry conditions. Journal of Geology, 80, 398–420.

Niizeki, N. and Wachi, M. (1968) The crystal structures of $Bi_2Mn_4O_{10}$, $Bi_2Al_4O_9$ and $Bi_2Fe_4O_9$. Zeitschrift für Kristallographie, 127, 173–187.

Peacor, D. (1967) Refinement of the crystal structure of pyroxene of formula M_IM_{II} $(Si_{1.5}Al_{0.5})O_6$. American Mineralogist, 52, 31–41.

Robie, R. A., Bethke, P. M., Toulmin, M. S. and Edwards, J. L. (1966) X-ray crystallographic data, densities, and molar volumes of minerals. In S. P. Clark, Ed., Handbook of Physical Constants p. 27–73. Geological Society of America Memoir, 97.

Robinson, K., Gibbs, G. V. and Ribbe, P. H. (1971) Quadratic elongation: A quantitative measure of distortion in coordination polyhedra. Science, 172, 567–570.

Ruby, S. L. (1973) Why misfit when you already have χ^2? Mössbauer Effect Methodology, 8, 263–276.

Sahama, T. G., Lehtinen, M., Rehtijärvi, P. and v. Knorring, O. (1974) Properties of sapphirine. Annales Academiae Scientiarum Fennicae, Series A, 3, 1–24.

Schreyer, W. (1965) Synthetische und natürliche Cordierite II. Die chemischen Zusammensetzungen natürlicher Cordierite und ihre Abhängigkeit von den PTX-Bedingungen bei der Gesteinsbildung. Neues Jahrbuch für Mineralogie, Abhandlungen, 103, 35–79.

Schreyer, W. and Seifert, F. (1970) Pressure dependence of crystal structures in the system MgO–Al_2O_3–SiO_2–H_2O at pressures up to 30 kilobars. Physics of the Earth and Planetary Interior, 3, 422–430.

Seifert, F. (1974) Stability of sapphirine: A study of the aluminous part of the system MgO–Al_2O_3–SiO_2–H_2O. Journal of Geology, 82, 173–204.

Seifert, F. and Olesch, M. (1977) Mössbauer spectroscopy of grandidierite, $(Mg,Fe)Al_3BSiO_9$. American Mineralogist, 62, 547–553.

Seifert, F. and Dasgupta, H. C. (1982) A note on the Mössbauer spectrum of ^{57}Fe in braunite. Neues Jahrbuch für Mineralogie, Monatshefte, 11–15.

Sharma, K. K., Langer, K. and Seifert, F. (1973) Some properties of spinel phases in the binary system $MgAl_2O_4$–$MgFe_2O_4$. Neues Jahrbuch für Minerabgie, Monatshefte, 442–449.

Steinfink, H. (1962) Crystal structure of a trioctahedral mica: phlogopite. American Mineralogist, 47, 886–896.

Steinwehr, H. E. v. (1967) Gitterkonstanten im System α-$(Al,Fe,Cr)_2O_3$ und ihr Abweichen von der Vegardregel. Zeitschrift Für Kristallographie, 125, 377–403.

Takéuchi, Y. (1965) Structures of brittle micas. Proceeding of the 13th National Conference on Clay and Clay Minerals, 1964, 1–25.

Tang Kai, A., Annersten, H. and Ericsson, T. (1980) Molecular orbital (MSXα) calculations of s-electron densities of tetrahedrally coordinated ferric iron: Comparison with experimental isomer shifts. Physics and Chemistry of Minerals, 5, 343–349.

Weber, H. P., Virgo, D. and Huggins, F. E. (1975) A neutron-diffraction and ^{57}Fe Mössbauer study of a synthetic Ti-rich garnet. Carnegie Institution of Washington Year Book, 74, 575–579.

Manuscript received, November 6, 1981
accepted for publication, June 28, 1983.